

Bond Distortion and Electron States in Charged C_{60}^{2-}

Rong Tang Fu^{*}, Rouli Fu[†], Kee Hag Lee^{†*}, Xin Sun^{**}, and Hong Juan Ye[‡]

[†]Department of Chemistry, WonKwang University, Iri 570-749

^{*}Department of Physics, Fudan University, Shanghai 200433, China

[‡]National Laboratory of Infrared Physics, Shanghai Institute of Technical Physics, Shanghai 200083, China

Received July 16, 1993

By considering both electron-electron and electron-lattice interactions, the effect of charge transfer on the bond structure and electronic states of C_{60} is studied without configuration limitation. The results show that the electron-electron interaction does not eliminate the layer structure of the bond distortion and the self-trapping of transferred electrons. For charged C_{60}^{2-} , there exist two localized electronic states, which possess laminar wave functions, and four nonequivalent groups of carbon atoms, which induce a fine-structure in the NMR spectrum line.

Introduction

One of the most prominent feature of fullerene is its relevance to the superconductivity¹⁻³. Although fulleride (solid C_{60}) itself is not superconductor, the doped fulleride M_3C_{60} with alkali metals $M=K, Rb, Cs$ becomes superconductor with fairly high transition temperature $T_c=18$ K for K_3C_{60} ¹, 28 K for Rb_3C_{60} ², and 33 K $RbCs_2C_{60}$ ³.

Since the ionization energy of alkali metals is lower than other elements in doped C_{60} , the electrons are easy to be transferred from the alkali metal to C_{60} . An interesting question is raised: where will the transferred electrons stay? Will they spread over the whole ball or be localized in some small area? Obviously the answer depends on the rigidity of C_{60} 's bonds as well as the competition between electron-lattice and electron-electron interactions. If the bonds are rigid, the transferred electrons will directly go to the lowest unoccupied molecular orbitals (LUMO), which wave functions are extended. Otherwise, if the bonds are soft enough, the lattice can be distorted by the transferred electrons to form some self-trapping states, then the electrons will be localized.

Recently several groups studied this problem⁴⁻⁸. Harigaya⁴ and Friedman⁵ find that the doped C_{60} can form string polaron, in which the dimerization is suppressed along a meridian. Fu *et al.*⁶ and Lee *et al.*⁷ find that both the bond distortion and self-trapping electron states possess layer structure with symmetry D_{3d} . Lee *et al.*⁷ further find that the bond distortion depends on electron-lattice interaction and can be D_{3d} , C_{2v} , or C_s . However, in these studies, only is the electron-lattice interaction considered, and the electron-electron interaction is neglected. Since the Coulomb repulsion usually resists electrons concentrating, and the electron-lattice interaction favors bond distortion and self-trapping, the competition between the electron-electron and electron-lattice interactions is an important fact to determine the formation of the self-trapping states. Coulon and his coworkers also studied this problem by using the local-spin density approximation of density functional method⁸. However, for the sake of simplifying the calculation, they limit the distortion to the configuration with symmetry D_{3d} , and it can't be verified that such configuration is more stable than others. Therefore, in order to answer the above question more reliably, it is nee-

ded to make two improvements: 1. Both electron-electron and electron-lattice interactions are considered, 2. The symmetry limitation imposed on the distortion should be lifted. Then the most stable distortion can be found. These improvements are carried out in the following section.

Formulation

In this paper, the electron-lattice interaction is described by the tight-binding model of π electrons with as bond-length dependent hopping coefficient h_{ij}

$$h_{ij} = h_0 + \alpha(d_{ij} - d_0) \quad (1)$$

where h_0 is the hopping constant, α the electron-lattice coupling, d_{ij} the bond length between the neighboring atoms sitting at \vec{r}_i and \vec{r}_j , and $d_0=1.54$ Å the bond length of diamond. Meanwhile the electron-electron interaction is depicted by the Hubbard model as follows:

$$\left(\frac{U}{2}\right) \sum_{i,s} \left(n_{i,s} - \frac{1}{2}\right) \left(n_{i,-s} - \frac{1}{2}\right) \quad (2)$$

Here $n_{is} = C_{is}^+ C_{is}$ where C_{is}^+ and C_{is} are creation and annihilation operators of electron at atom i with spin s , and the interaction parameter U is taken to be h_0 .

By using the unrestricted Hartree-Fock approximation for the electron-electron interaction, the Hamiltonian is given by

$$H = - \sum_{i,s} h_{ij} (C_{i,s}^+ C_{j,s} + h.c.) + \frac{K}{2} \sum_{ij} (d_{ij} - d_0)^2 + U \sum_{i,s} \left(X_{i,s} - \frac{1}{2}\right) C_{i,s}^+ C_{i,s} - \frac{U}{2} \sum_{i,s} X_{i,s} X_{i,-s} \quad (3)$$

Here K is the elastic constant and

$$X_{i,s} = \langle C_{i,-s}^+ C_{i,-s} \rangle. \quad (4)$$

We follow the method described in Ref. 9 to calculate self-consistently the electron states and lattice distortion.

The eigen-equation of the Hamiltonian (3) is

$$\epsilon_n^s Z_{i,n}^s = - \sum_j h_{ij} Z_{j,n}^s + U \left(X_{i,s} - \frac{1}{2}\right) Z_{i,n}^s \quad (5)$$

where ϵ_n^s and $Z_{i,n}^s$ are n -th energy level and wave function.

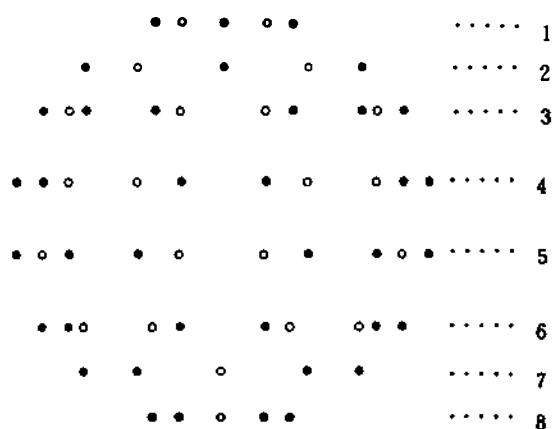


Figure 1. Layer structure of C_{60} . Here the numerals in the right column indicate the layer's numbers.

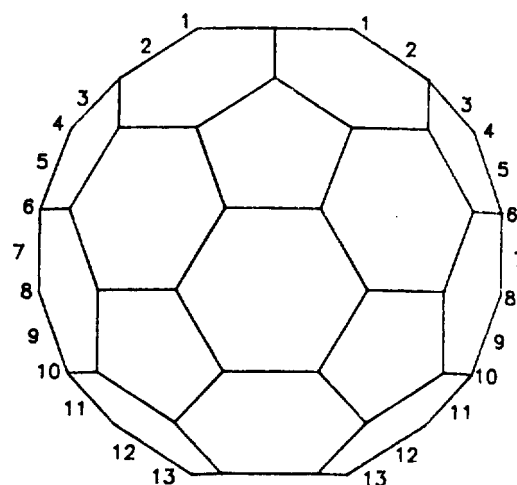


Figure 2. Bond structure of C_{60} . Here the numbers of the bond-layers are indicated by the numerals.

The total energy is

$$E = \sum_{n'} \epsilon_n^2 - \frac{U}{2} \sum_{n,s} X_{n,s} X_{n,-s} + \frac{K}{2} \sum_{ij} (d_{ij} - d_0)^2. \quad (6)$$

The stable distorted configuration of carbon atoms is determined by minimizing the total energy in Eq. (6) with respect to the atom's position \vec{r}_i . In this step, we do not impose any limitation on the configuration variation. It is different from Ref. 8, where the distortion configuration was limited in the symmetry D_{3d} . When we consider the charged C_{60} with two transferred electrons, the computation is reduced by the spin symmetry.

Before studying the bond distortion and self-trapping caused by the charge transfer, the parameters h_0 , α and K should be figured out first. This can be done by fitting the experimental data of the pristine C_{60} . The X-ray diffraction¹⁰ shows that the pentagon edge (long bond) is 1.432 Å and the hexagon-hexagon border (short bond) is 1.388 Å, and the NMR¹¹ gives the long bond 1.45 ± 0.015 Å and short bond 1.40 ± 0.015 Å. Meanwhile the photoemission¹² shows the energy separation between LUMO and HOMO is about 1.9 eV. Our numerical calculation tells that when $h_0 = 1.8$ eV, $\alpha = 3.5$ eV/Å, and $K = 60.0$ eV/Å² in the case of 60 electrons, the resultant long-bond length is 1.432 Å, the short one is 1.395 Å and the level of the LUMO is 1.85 eV higher than the HOMO. These theoretical values are very close to the experimental data.

Bond distortion and self-trapping

The stable configuration of the charged C_{60}^{2-} can be obtained by minimizing the energy in Eq. (6) with 62 electrons. Since we do not impose any limitation on the distortion, the resultant configuration should be the most stable structure of the C_{60}^{2-} . Then it is possible to tell what symmetry the charged C_{60}^{2-} should have.

Our results show that, after the electron-electron interaction is switched on, there still exist two self-trapping electronic states localized in equator area, and both the bond distortion and the wave functions of self-trapping states remain to have the layer structures. It means that the electron interaction does not eliminate the self-trapping and layer

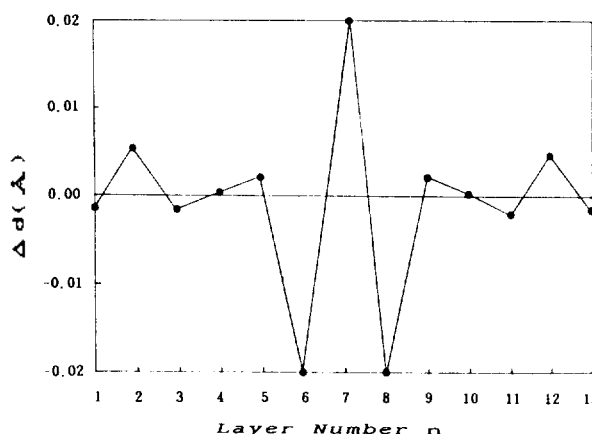


Figure 3. Layer-dependent changes of bond lengths of charged C_{60}^{2-} .

structure. The features of the bond distortion and self-trapping can be distinctly displayed if the buckyball is oriented in such a way that its top and bottom are pentagons, which is shown in Figure 1 where the dots are in the front side of the ball and the circles in the back side.

In this disposal, the Buckyball apparently consists of eight layers. Meanwhile the 90 bonds are divided into 13 layers as shown in Figure 2.

The pristine C_{60} has dimerization structure with only two kinds of bonds, the long bond and short bond. Such dimerization structure is distorted by the transferred electrons: some bonds are stretched and others shrunk. The bond distortion possesses the following features:

1. The bonds in the same layer have same change in their bond lengths. The layer-dependent changes of the bond length are shown in the Figure 3.

2. For the distorted bond structure, the upper half and lower half have inversion symmetry.

3. The changes of the bond length in the middle layers are much larger than the other layers. It means that the bond distortion is localized in the equator area.

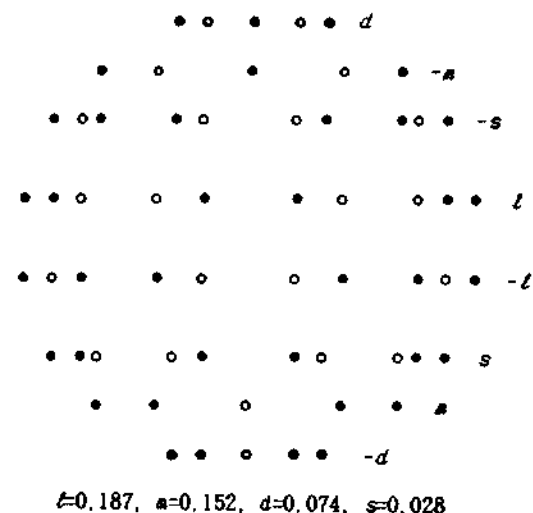
The first two features indicate that the charged C_{60}^{2-} pos-

Table 1. Energy levels E_k , molecular orbitals k and degeneracies g_k of pristine C_{60} and charged C_{60}^{2-}

C_{60}			C_{60}^{2-}		
$E_k(\text{eV})$	k	g_k	$E_k(\text{eV})$	k	g_k
6.7350	T_{2g}	3	6.7874	A_{2g}	1
			6.7857	E_{2g}	2
6.6082	G_u	4	6.6617	E_{2u}	2
			6.6582	E_{1u}	2
5.3464	G_g	4	5.4057	E_{2g}	2
			5.4015	E_{1g}	2
4.4869	H_u	5	4.5757	A_{1u}	1
			4.5515	E_{2u}	2
			4.5301	E_{1u}	2
4.0522	T_{2u}	3	4.1435	E_{2u}	2
			4.0898	A_{2u}	1
3.7470	H_g	5	3.8333	E_{2g}	2
			3.8178	E_{1g}	2
			3.8067	A_{1g}	1
1.8615	T_{1g}	3	1.9279	A_{2g}	1
			1.8598	E_{1g}	2
1.3191	T_{1u}	3	1.3740	E_{1u}	2
(LUMO)			(LUMO)		
			1.2729	A_{2u}	1
			(HOMO)	$[\psi(a_{2u})]$	
-0.5074	H_u	5	-0.3372	A_{1u}	1
(HOMO)				$[\psi(a_{1u})]$	
			-0.4563	E_{2u}	2
			-0.4610	E_{1u}	2
-1.3237	H_g	5	-1.2225	E_{2g}	2
			-1.2547	E_{1g}	2
			-1.2849	A_{1g}	1
-1.3669	G_g	4	-1.2930	E_{2g}	2
			-1.3237	E_{1g}	2
-2.6287	G_u	4	-2.5319	E_{2u}	2
			-2.5620	E_{1u}	2
-3.0846	T_{2u}	3	-3.0394	E_{2u}	2
			-3.0517	A_{1u}	1
-4.2114	H_g	5	-4.1391	E_{2g}	2
			-4.1527	A_{1g}	1
			-4.1610	E_{1g}	2
-5.2251	T_{1u}	3	-5.1588	E_{1u}	2
			-5.1690	A_{2u}	1
-5.7675	A_g	1	-5.7039	A_{1g}	1

sesses the symmetry D_{5d} . So our calculation proves that the distortion with the symmetry D_{5d} is the most stable.

The distortion of bond structure brings about some observable effects. One is the fine-structure of the NMR spectrum line. In pristine C_{60} all the 60 carbon atoms are equivalent and the spectrum of NMR has only one line at 142.68 ppm¹³. Now the bond structure of charged C_{60}^{2-} is distorted and the atoms are no longer equivalent. However the bond distortion does not completely destroy the equivalence of the atoms. Since the bond distortion has D_{5d} symmetry, the atoms in the first and eighth layers (shown on Figure 1)

**Figure 4.** Self-trapping state $\psi(a_{2u})$. Here the number in each site indicates the value of the wave function $\psi(a_{2u})$.

are equivalent to each other. Similarly, the atoms in the second and seventh layers, third and sixth, fourth and fifth are equivalent respectively. Hence, there are four groups of atoms in charged C_{60}^{2-} . The numbers of atoms in these four groups are 10, 20, 20, 10. Since the atoms in different groups are nonequivalent, the spectrum in the NMR of charged C_{60}^{2-} should have a fine-structure with 4 sublines, whose intensity ratio is 1:2:2:1. Since the resolution of NMR can reach 10^{-2} ppm, it is good enough to find the fine-structure.

The above distortion reduces the symmetry from I_h to D_{5d} and, accordingly, lifts some degeneracies.

The detail of the level splits is given in Table 1, where the left part is the pristine C_{60} , the right part is charged C_{60}^{2-} ; E_k denotes energy level, k the representation of molecular orbital, g_k degeneracy. It can be seen from this table that, except the HOMO and the LUMO, the splits of C_{60} after the charge transfer are very small. However, the splits in the HOMO and the LUMO much bigger. The five-fold degenerate HOMO level H_u is split into three levels E_{1u} , E_{2u} and A_{1u} . Both E_{1u} and E_{2u} are two-fold degenerate and close to each other. But the state A_{1u} , which wave function is denoted as $\psi(a_{1u})$, is apparently raised up to 0.12 eV. At the same time, the three-fold degenerate LUMO level T_{1u} is split into two levels E_{1u} and A_{2u} . E_{1u} is two-fold degenerate and A_{2u} , which wave function denoted as $\psi(a_{2u})$, is apparently pulled down to 0.1 eV. It means that the distortion produces only two states $\psi(a_{2u})$ and $\psi(a_{1u})$ which levels are distinctly shifted from the original levels. These two states possess some peculiar characteristics:

1. Both $\psi(a_{2u})$ and $\psi(a_{1u})$ have layer structures. Their wave functions are shown in Figure 4 and 5. In each layer, different sites have the same absolute value of the wave function. Such layer structure is understandable, since these two states are produced by the bond distortion, and the bond distortion itself has layer structure. Due to the symmetry σ_d , these two states have a symmetry plane through the polar axis. Here the polar axis means C_5 axis in the D_{5d} point group. With respect to this plane, $\psi(a_{1u})$ is antisymmetric and $\psi(a_{2u})$

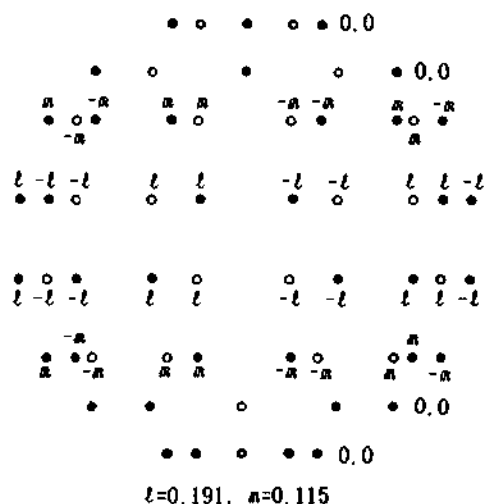


Figure 5. Self this-trapping state $\psi(a_{1u})$. Here the number in each site indicates the value of the wave function $\psi(a_{1u})$.

symmetric.

2. These two states are localized in the equator area.

These features manifest that $\psi(a_{2u})$ and $\psi(a_{1u})$ are the self-trapping electronic bound states associated with the bond

distortion induced by the charge transfer.

Acknowledgement. This work was supported by the Korea Science and Engineering Foundation and the National Science Foundation of China.

References

1. A. Hebard, *Nature* **350**, 600 (1991).
2. (a) K. Holczer, *et al.*, *Science* **252**, 1154 (1991); (b) M. Rossensky, *et al.*, *Phys. Rev. Lett.* **60**, 2830 (1991).
3. K. Tanigaki, *et al.*, *Nature* **352**, 222 (1991).
4. K. Harigaya, *Phys. Rev.* **B45**, 13676 (1992).
5. B. Friedman, *Phys. Rev.* **B45**, 1454 (1992).
6. R. T. Fu, R. L. Fu, X. Sun, and Z. Chen, *Chinese Phys. Lett.* **9**, 541 (1992).
7. K. H. Lee and U.-H. Paek, *J. Phys. Chem. Solids*, **54**, 565 (1993).
8. V. de Coulon, J. L. Martins, and F. Reuse. *Phys. Rev.* **B45**, 13671 (1992).
9. C. Q. Wu and X. Sun, *Phys. Rev.* **B33**, 8772 (1986).
10. J. M. Hawkins, *et al.*, *Science* **252**, 312 (1991).
11. C. S. Yannoni, *et al.*, *J. Am. Chem. Soc.* **113**, 3190 (1991).
12. J. H. Weaver, *Phys. Rev. Lett.* **66**, 1741 (1991).
13. (a) R. Taylor, *et al.*, *J. Chem. Soc. Chem. Commun.* 1423 (1990); (b) H. Ajie, *et al.*, *J. Phys. Chem.*, **94**, 8641 (1990).

Selective Reduction by Lithium Bis- or Tris(dialkylamino)aluminum Hydrides. VII. Reaction of Lithium Tris(dihexylamino)aluminum Hydride with Selected Organic Compounds Containing Representative Functional Groups¹

Jin Soon Cha*, Oh Oun Kwon, and Jae Cheol Lee

Department of Chemistry, Yeungnam University, Kyongsan 712-749

Received July 23, 1993

The approximate rates and stoichiometry of the reaction of excess lithium tris(dihexylamino)aluminum hydride(LTDHA) with selected organic compounds containing representative functional groups under the standardized conditions (tetrahydrofuran, 0°C) were studied in order to define the reducing characteristics of the reagent for selective reductions. The reducing ability of LTDHA was also compared with those of the parent lithium aluminum hydride(LAH), lithium tris(diethylamino)aluminum hydride(LTDEA), and lithium tris(dibutylamino)aluminum hydride(LTDBA). In general, the reactivity toward organic functionalities is in order of LAH>LTDEA>LTDBA>LTDHA. LTDHA shows a unique reducing characteristics. Thus, the reagent reduces aldehydes, ketones, esters, epoxides, and tertiary amides readily. Anthraquinone is cleanly reduced to 9,10-dihydro-9,10-anthracenediol without hydrogen evolution, whereas *p*-benzoquinone is inert to LTDHA. In addition to that, disulfides are also readily reduced to thiols without hydrogen evolution. However, carboxylic acids, anhydrides, nitriles, and primary amides are reduced slowly. Especially, this reagent reduces aromatic nitriles to the corresponding aldehydes in good yields.

Introduction

Lithium aluminum hydride (LAH), a very powerful reducing agent, has been widely used for the reduction of functional groups.² The introduction of alkoxy groups into lithium

aluminum hydride^{3,4} modifies its reducing characteristics⁵⁻⁸ and has made possible a number of selective reductions of considerable utility in synthetic work.⁹

Similarly, the dialkylamino-substituted derivatives of lithium aluminum hydride seem to exhibit reducing properties